*High Voltage*

WILEY

国家电网 STATE GRID 中国电力科学研究院有限公司 CHINA ELECTRIC POWER RESEARCH INSTITUTE | IET The Institution of Engineering and Technology

ORIGINAL RESEARCH OPEN ACCESS

# Bioactive Anti-Inflammatory and Antibacterial Plasma-Activated Air for Healing of Infected Wounds

Xixi Jing[1] | Zizhu Zhang[1] | Fugao Zhang[1,2] | Zijin Wu[1] | Dingxin Liu[1] | Hao Zhang[1,3] | Yilin Wang[4] | Jishen Zhang[1] | Zifeng Wang[1] | Li Guo[1] | Mingzhe Rong[1] | Paul K. Chu[5]

[1]State Key Laboratory of Electrical Insulation and Power Equipment, Centre for Plasma Biomedicine, Xi'an Jiaotong University, Xi'an, China | [2]Power Dispatching Control Center of Guizhou Power Grid Co. Ltd, Guizhou, China | [3]Frontier Institute of Science and Technology, Xi'an Jiaotong University, Xi'an, China | [4]Department of Orthopedics and Traumatology, Peking University People's Hospital, Beijing, China | [5]Department of Physics, Department of Materials Science and Engineering, and Department of Biomedical Engineering, City University of Hong Kong, Hong Kong, China

**Correspondence:** Hao Zhang (zhang216@mail.xjtu.edu.cn)

**Received:** 7 May 2024 | **Revised:** 15 July 2024 | **Accepted:** 19 July 2024

**Associate Editor:** Chenguo Yao

**Funding:** This study was supported by National Natural Science Foundation of China (Grant 52277231); City University of Hong Kong Donation Research (Grant DON-RMG 9229021); Hong Kong PDFS—RGC Postdoctoral Fellowship Scheme (PDFS2122-1S08).

## ABSTRACT

Cold atmospheric plasmas are widely used in biomedicine. Although direct plasma treatments of wounds have been demonstrated, there are still obstacles hampering further clinical adoption, for example, the limited treatment area, inconsistent actions and risk of thermal injury. In this respect, plasma-activated air (PAA) is proposed and demonstrated for infected wounds treatment as an alternative to the conventional direct plasma treatment. The combination of gliding arc discharge reactor and dielectric barrier discharge reactor produces highly bioactive PAA. In in vitro sterilisation of *Staphylococcus aureus*, approximately 9-log reduction is achieved after the PAA treatment for 6 min. Bovine serum albumin is added to the *S. aureus* suspension to further simulate the wound exudate to accomplish inactivation of approximately 3-log reduction after 10 min. In vivo experiments show that the PAA treatment of infected wounds significantly reduces the bacterial load and improves the healing rate, revealing an optimal treatment time of 3 min/day. The immunohistochemical and blood biochemical analyses show that the PAA-3 min treatment enhances wound healing by inhibiting the tissue inflammatory response and inducing growth factor production without showing evident systemic toxicity. In conclusion, PAA holds great clinical promise as a safe and effective wound-healing strategy.

## 1 | Introduction

Wound healing is an intricate process that involves synergistic actions of diverse cells, cytokines and growth factors. It consists of four phases: haemostasis, inflammation, proliferation and remodelling [1, 2]. Colonisation of microorganisms during wound healing causes infections, further prolonging and exacerbating the inflammatory phase, thereby delaying the process of wound healing and leading to chronic wounds [3]. Poorly healed chronic wounds impose a considerable impact on the patients, thereby leading to high mortality rates [4, 5]. Currently, chronic wounds are usually treated with antimicrobial dressings after wound debridement, and antibiotics are used to control bacterial infections [6]. However, these traditional methods still have problems related to limited healing and antibacterial capabilities as well as antibiotic resistance [7]. Therefore, new wound therapies are urgently needed, and their development must ensure adequate biocompatibility, antibacterial and anti-inflammatory properties in addition to quick promotion of healing at the wound sites [8].

The cold atmospheric plasma (CAP) is a partly ionised gas produced at near-ambient temperature and pressure. It consists of a complex mixture of electrons, ions, free radicals, photons, electrically neutral atoms and ultraviolet radiation and can also deliver an intense transient electric field [9, 10]. Additionally, their combined action has led to a wide range of biomedical applications of CAP technology, including sterilisation [11], disinfection [12], cancer therapy [13, 14], skin diseases [15, 16] and drug delivery [17]. Dielectric barrier discharge and plasma jet have been developed in wound treatment, and the potential of CAP in the area of wound healing has been illustrated in the relevant studies [18, 19]. Plasma-generated reactive species such as reactive oxygen species (ROS) and reactive nitrogen species (RNS) are considered to play key roles in wound healing [20]. ROS and RNS such as $H_2O_2$, OH and NO are the natural wound-healing components. The actions of exogenous reactive species produced by CAP are well tolerated and more effective for wound treatment. On the one hand, CAP-produced reactive species promote wound healing by inactivating bacteria and reducing the bacterial load on the wound. Plasma sterilisation has the advantages of high efficiency, safety and broad spectrum. Studies have shown that CAP can sterilise in an appropriate dose range without harming human cells [21]. In addition, CAP has good in vitro and in vivo sterilisation effects against more than 100 clinically isolated wound bacteria including drug-resistant bacteria [22, 23].

On the other hand, partially CAP-produced reactive species can give rise to tissue regeneration to promote wound healing. It is well known that $H_2O_2$ and OH are involved in blood coagulation and promote wound contraction by mediating the growth factors [24]. NO, as a typical representative of RNS, plays a key role in anti-inflammation, maintaining vascular homoeostasis, promoting new blood vessel formation and tissue remodelling [25]. However, although CAP has great potential in direct wound treatment, the inherent characteristics of the discharge plasma also lead to problems such as the undersized treatment area, uneven treatment and risk of thermal injury, consequently limiting the clinical development of CAP for wound treatment. In addition, plasma jet requires an inert gas as the working gas, which increases the size and cost of equipment development compared to air discharge plasma. Therefore, plasma wound treatments need further improvement to meet practical medical needs.

Herein, plasma-activated air (PAA) is proposed as a potential alternative therapy for infected wounds. It is generated by a novel combination of the gliding arc discharge reactor and dielectric barrier discharge reactor with air as the working gas. The PAA therapy circumvents the limitations of direct plasma treatments while generating more ROS and RNS, especially high-valent $NO_x$ and NO, which play key roles in antimicrobial and wound contraction [26, 27]. The *Staphylococcus aureus* suspension is used to access the in vitro sterilisation effects of PAA and the effects are demonstrated by an infected rat wound model. The effects of PAA on the infected wound healing are evaluated, and the mechanisms of wound healing are analysed by immunohistochemical and immunofluorescence staining. Finally, the safety of PAA applied to rats is evaluated by blood examination and histological analysis of the vital organs.

## 2 | Materials and Methods

### 2.1 | Experimental Setup and Measurement of Reactive Species

In this study, the gliding arc discharge reactor and DBD discharge reactor were connected in series, as opposed to the conventional parallel connection method, as shown in Figure 1. The gliding arc discharge reactor was composed of two oppositely placed stainless steel blades (minimum distance = 1 mm and blade length = 30 mm) and an air nozzle (inner

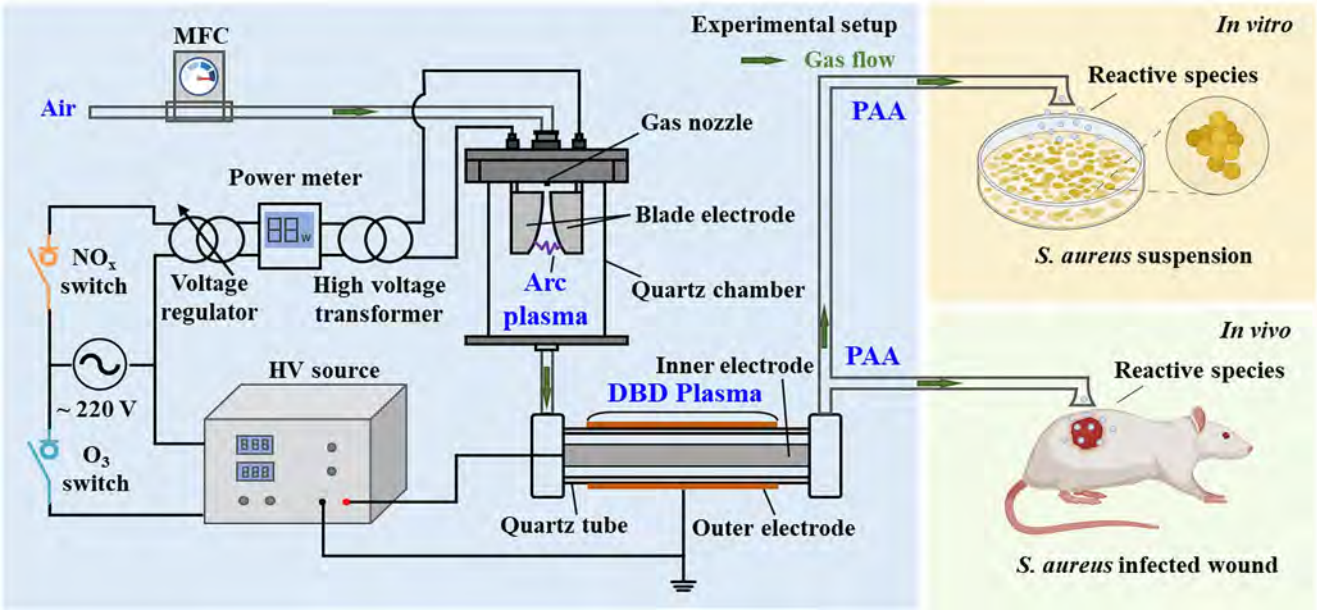


**FIGURE 1** | Experimental setup for the generation of plasma-activated air (PAA) using the gliding arc discharge plasma and dielectric barrier discharge (DBD) plasma (created with BioRender.com).

diameter = 1 mm) driven by a high-voltage transformer (Sinolift, TH5NT-1530) at a discharge power of approximately 30 W [25]. The DBD reactor was designed with a coaxial structure, and a stainless-steel bar (outer diameter = 14 mm) was coaxially placed in a quartz tube (outer diameter = 18 mm, thickness = 1 mm) to form the high-voltage electrode. A copper foil was a ground electrode (length = 150 mm) covering the outer periphery of the quartz tube. The DBD was driven by a high-voltage power supply (Suman, CTP-2000K) with the discharge power maintained at approximately 30 W. The synthetic air flow rate through both the gliding arc discharge reactor and DBD reactor was 5 standard litre per minute (SLM). The voltage supply and discharge current of the gliding arc discharge and DBD are depicted in Figure 2.

During the generation of CAP, gas molecules undergo a series of physicochemical processes such as collision, ionisation and excitation under the action of a high-voltage electric field, resulting in the formation of a large number of gaseous reactive species. Since the treated objects in biomedical applications are generally covered by a liquid layer, the gaseous reactive species need to contact the liquid phase and be converted into aqueous reactive species before acting on the lesions to produce the effects [28]. To detect the gaseous reactive species in PAA, a Fourier transform infrared (FTIR) spectrometry (Bruker, Tensor II) was performed with a 2.4-m optical path gas cell (Pike). The concentrations of the gaseous reactive species were determined according to the Lambert–Beer law, and the absorption cross-sections were derived from the HITRAN database [29]. To analyse the aqueous reactive species generated by PAA, a hydrogen peroxide assay kit (Beyotime) and nitrate/nitrite colourimetric assay kit (Beyotime) were used to measure the concentrations of $H_2O_2$, $NO_2^-$ and $NO_3^-$ on a multifunctional microplate reader (Thermo, Varioskan Flash). TEMPONE-H (Enzo) and MGD (Enzo) were used to measure the concentrations of $O_2^-$, $ONOO^-$ and NO by electron spin resonance (Bruker, EMXplus) [30].

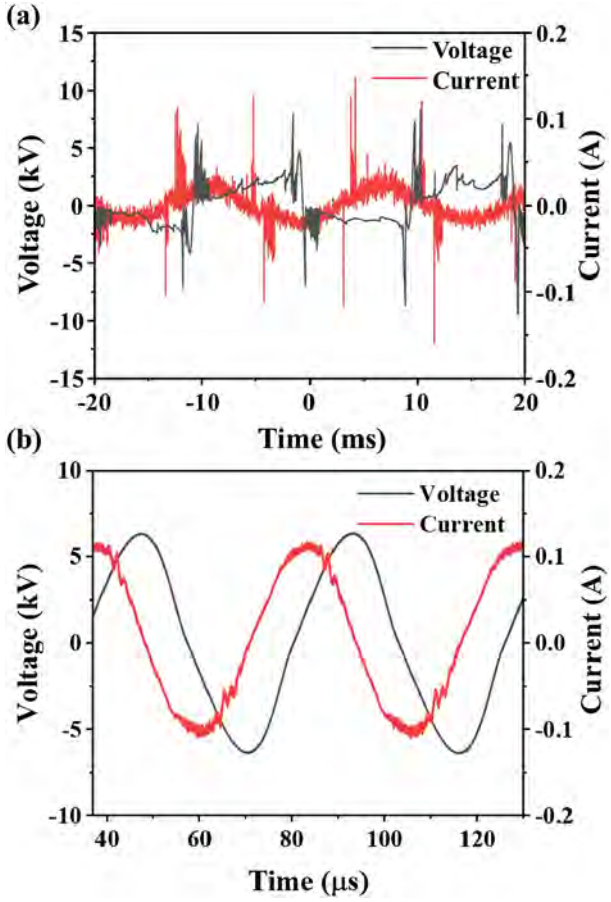


**FIGURE 2** | Voltage and discharge current waveforms: (a) gliding arc discharge plasma and (b) dielectric barrier discharge plasma.

## 2.2 | Evaluation of In Vitro Sterilisation Effects of PAA

During the initial stages of wound infection, gram-positive organisms such as *S. aureus* (CGMCC25923) are the dominant microorganisms, and bacterial concentrations exceeding $10^5$ or $10^6$ colony-forming units per gram of tissue impede wound healing [31–33]. Here, *S. aureus* was chosen to study the sterilisation effects in vitro and wound anti-infection effects in vivo. The *S. aureus* medium was prepared as described previously [34], and the optical density (OD) value at 600 nm was resuspended to approximately 1 ($10^8$ CFU/mL). The *S. aureus* suspension (500 μL) was placed in a 24-well plate and then treated by PAA. After standing for 10 min, 100 μL of the treated bacterial suspension was mixed with 900 μL of the phosphate-buffered saline (PBS). It was diluted 10 times sequentially and each gradient (10 μL) was placed in the tryptic soy broth (TSB) solid medium. After the bacterial mixture was absorbed by TSB, TSB plates were placed in an incubator at 37°C for 24–48 h before the colonies were counted to calculate the number of surviving bacteria.

## 2.3 | Infected Wound Models and PAA Treatment

The female Sprague Dawley (80 ± 5) g rats were raised in the Laboratory Animal Center of Xi'an Jiaotong University (Xi'an, China). In this study, all the experimental operations were performed in accordance with animal welfare guidelines approved by the Ethics Committee (No. xjtu2022-1109). Before constructing the wound model, each rat was injected with the pentobarbital sodium anaesthetic with a concentration of 1% (weight/volume) according to the body weight. After the rats were anaesthetised, the back hair was removed with a rat-specific shaver and depilatory cream. The sterile scissor was used to cut a circular wound with a diameter of 2 cm on the back of the rat, and the suspension of *S. aureus* (200 μL) ($OD_{600} \approx 10$, $9 \times 10^9$ CFU/mL) was inoculated into the wound to induce wound infection. One hundred wound model rats were randomly divided into 4 groups (control, 3 min PAA, 6 min PAA and 10 min PAA treatment group). Three hours after wound modelling, the wounds were treated with PAA, as shown in Figure 1, and wound treatments were performed at the same time every day thereafter.

## 2.4 | Wound Healing Analysis

The wounds were photographed every 2 days from the first day (the day of wound introduction) with a ruler placed next to each

rat as a reference by a camera (Nikon D7000, exposure time of 1/30 s) placed at the same height every time. All the operations were performed by the same person for consistency. The wounds were processed by the ImageJ software. To assess the bacterial load in the wounds, five rats were randomly selected from each group and euthanised by cervical dislocation on the 2nd and 4th day of wound healing. The wound tissues were cut with sterile scissors, placed in 1.5 mL PBS buffer solution, and ground with a tissue grinder (Shanghai Jingxin, JXSTPRP-L) for 10 min at a frequency of 60 Hz. The surviving bacteria were then counted using the method described above.

### 2.5 | Immunohistochemical and Immunofluorescence Staining Analyses

On the 6th day of wound healing, five rats from each group were randomly selected and euthanised by cervical dislocation. The wound tissues were cut with sterile scissors and immediately fixed in 4% paraformaldehyde. The fibroblast growth factor (FGF), epidermal growth factor (EGF) and vascular endothelial growth factor (VEGF) were determined by immunohistochemical analyses, and the macrophage content was analysed by immunofluorescence staining with CD68 antibody (Wuhan Seville Biotechnology Company, China).

### 2.6 | Biosafety Analysis of PAA

The weights of the rats were recorded regularly, and their behaviour and health status were observed. On the 6th day, three rats from each group were randomly selected and euthanised by cervical dislocation, and blood was quickly taken from the heart with a syringe for analysis. The haematological analysis was performed for the following parameters: white blood cells (WBC), lymphocytes (Lymph), monocytes (Mon), granulocytes (Gran), red blood cells (RBC), haemoglobin (HGB), haematocrit (HCT), mean corpuscular volume (MCV), mean corpuscular haemoglobin (MCH), mean corpuscular haemoglobin concentration (MCHC), red cell distribution width (RDW), platelets (PLT), mean platelet volume (MPV), plateletcrit (PCT), platelet distribution width (PDW) and platelet distribution width (PDW). The heart, liver, spleen, lung and kidney were removed and fixed in 4% paraformaldehyde after dissecting for H&E staining. The blood and visceral tissue samples were sent to Wuhan Seville Biotechnology Company (Wuhan, China) for testing.

### 2.7 | Statistical Analysis

All experiments were repeated at least three times. The experimental data were presented as the means ± standard deviations. Statistical significance was determined using a two-tailed *t*-test, with *p* values indicating the level of significance. Differences between two independent groups were considered statistically significant when $p < 0.05$ (ns = no significance, $^{*}p < 0.05$, $^{**}p < 0.01$, $^{***}p < 0.001$).

## 3 | Results and Discussion

### 3.1 | Reactive Species in PAA and Antibacterial Properties In Vitro

The FTIR spectra of PAA in Figure 3 show that the primary gaseous reactive species generated by the gliding arc discharge were low-valence NO and $NO_2$ ($NO_x$-gas). The low-valence $NO_x$ was produced by the dissociation of $N_2$ and $O_2$ molecules in air, whereas the production of $O_3$ was suppressed by the high temperature of the gliding arc [35]. The main reactive species of the DBD reactor was $O_3$ ($O_3$-gas), which was formed because of the easier dissociation of $O_2$ and lower energy threshold than $N_2$ [36]. The $NO_x$-gas generated by the gliding arc discharge reactor was vented into the DBD reactor for further discharge (mixed gas), NO was oxidised by $O_3$ to $NO_2$, $NO_2$ was further oxidised by $O_3$ to $NO_3$ and then $N_2O_5$ was produced by the combination of $NO_2$ and $NO_3$ [26]. In the combined gliding arc reactor and DBD reactor, the gaseous products of NO, $NO_2$ and $O_3$ coexist in large quantities and finally produce high-valence $NO_x$, especially $N_2O_5$, with higher antimicrobial activity [37]. Therefore, PAA (mixed gas) was used for further wound healing studies.

Exudates often exist on the surface of early infected wounds and in order to explore the interactions between PAA and wound exudates, the penetration and accumulation of aqueous reactive species in saline (as an alternative to exudate) after the PAA treatment are investigated. The high-valence $NO_x$ in PAA, such as $N_2O_5$, reacts in an aqueous solution to produce a variety of aqueous ROS and RNS such as $H_2O_2$, NO, $NO_2^-$, $NO_3^-$, $O_2^-$ and $ONOO^-$, as expressed in reactions (1)–(8) shown in Table 1 [38, 39].

As shown in Figure 4a–d, the concentrations of ROS and RNS in the PAA-treated saline increase with the treatment time.

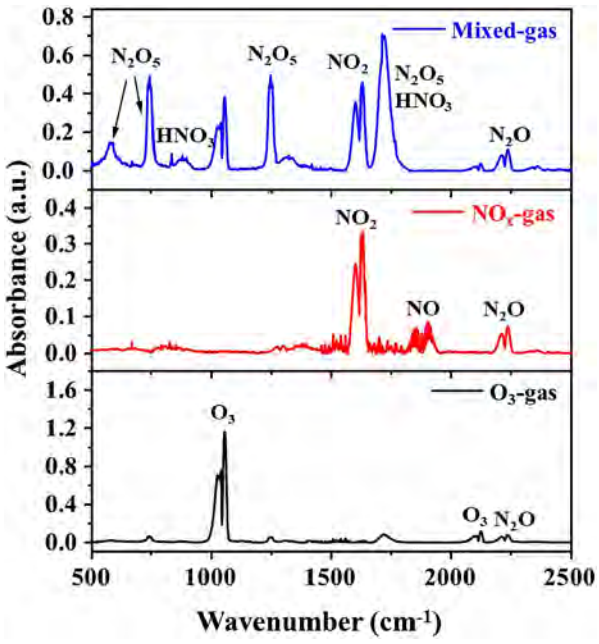


**FIGURE 3** | FTIR spectra of PAA with the dielectric barrier discharge plasma-activated air denoted as $O_3$-gas, gliding arc discharge plasma-activated air denoted as $NO_x$-gas and the combination of $O_3$-gas and $NO_x$-gas denoted as mixed gas.

**TABLE 1** | Liquid reactions.

| Reaction | Number |
|---|---|
| $NO_2+\cdot O\rightarrow NO+O_2$ | (1) |
| $NO_2+O_3\rightarrow NO+2O_2$ | (2) |
| $N_2O_5+H_2O\rightarrow 2ONOOH$ | (3) |
| $ONOOH\leftrightarrow ONOO^-+H^+$ | (4) |
| $ONOO^-\leftrightarrow NO+O_2^-$ | (5) |
| $N_2O_5+H_2O\rightarrow NO_3^-$ | (6) |
| $2NO_2+H_2O\rightarrow NO_2^-+NO_3^-+2H^+$ | (7) |
| $2\cdot OH\rightarrow H_2O_2$ | (8) |

After 10 min of PAA treatment, the concentrations of long-lived $NO_3^-$, $NO_2^-$ and $H_2O_2$ increase from about 0 μM to 232.0 mM, 917.9 and 119.1 μM, respectively, and those of short-lived $ONOO^-$ and $O_2^-$ increase from 0 to 67.8 μM. The detection result of aqueous NO is shown in Figure 4e, and the increase in the electron spin resonance (ESR) signal shows that NO is produced in the liquid phase after the PAA treatment. The CAP treatment of infected wounds is achieved by depositing exogenous reactive species locally into wound exudates and tissues and triggering ROS and RNS-mediated bacterial inactivation and tissue regeneration. Specifically, $ONOO^-$ and $O_2^-$ have been widely reported to be strong bactericidal reactive species [40, 41], which can reduce the bacterial load of wounds and thereby control wound infection. NO modulates the inflammatory response and causes vasodilation, increasing blood flow and tissue oxygenation [25, 42]. Here, PAA, as an alternative to CAP, can also accumulate various ROS and RNS on the wound surface after interacting with exudates similar to the CAP treatment wound directly, thereby having efficient antibacterial and pro-healing effects in wound therapy.

The *S. aureus* suspension was used to evaluate the sterilisation effects of PAA in vitro. After the PAA treatment for different durations, the growth of *S. aureus* on the TSB solid medium is shown in Figure 5a. Statistical results revealed that PAA treatment for 3 min resulted in approximately 4-log reductions from an initial CFU count of approximately 10 logs. When the treatment duration was extended to 6 min or 10 min, the reduction increases to approximately 9 logs, with bacterial counts falling below the detection limit, as shown in Figure 5b. To simulate the impact of wound blood and exudates on PAA sterilisation, bovine serum albumin (BSA, 6%) was added to the bacterial suspension. The presence of BSA significantly diminished the antibacterial efficacy of PAA. Specifically, after 3 min of PAA treatment, only 68.4% of the bacteria were inactivated, and after 10 min of treatment, approximately 3-log reduction was achieved from an initial CFU count of approximately 10 logs. Since the antibacterial effects of PAA on the *S. aureus* suspension are achieved by aqueous ROS and RNS accumulation, the amino acids and proteins in BSA can consume a portion of ROS and RNS [43, 44]. This may be why the antibacterial effect of PAA is significantly weakened after BSA addition. Although PAA has effective antimicrobial properties, its actions for an anti-infective treatment of wounds will be weakened to a certain extent by wound exudates or blood in vivo.

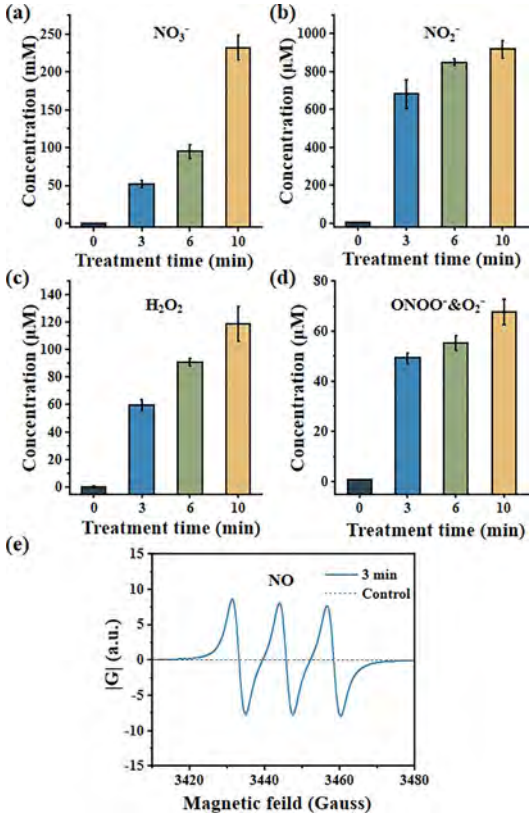


**FIGURE 4** | Aqueous ROS and RNS levels for different PAA treatment times: (a–d) concentrations of $NO_3^-$, $NO_2^-$, $H_2O_2$, $ONOO^-$ and $O_2^-$ and (e) electron spin resonance (ESR) spectra of MGD for NO capture.

## 3.2 | Antibacterial, Anti-Inflammatory and Wound Pro-Healing Effects of PAA In Vivo

In order to assess the therapeutic efficacy of PAA on infected wounds, the changes in the wound area are monitored based on a rat model with *S. aureus* on infected wounds after the PAA treatment. As shown in Figure 6a, after the 2-cm diameter circular wound was moulded, the wound areas of the rats in all the groups decrease with postoperative time, and there is an obvious dose-dependent effect on promoting wound healing. The rats treated with PAA for 3 min/time every day show the best wound healing effects. The wounds scab rapidly and shrink to about 50% of that of the control group (without treatment) after 4 days. The infected wounds basically heal on the 12th day. In the group treated with PAA for 6 min, wound healing was not as effective as the PAA-3 min group, and the wound area is about 80% of that of the control group during the first 8 days (Figure 6b). When the treatment time is extended to 10 min, there is a certain inhibitory effect on wound healing compared to the control group, showing that excessive reactive species in PAA are detrimental to wound healing. These results indicate that only an appropriate dose of PAA can promote infected skin wound healing in rats.

The wound healing process is quite complex, and bacterial colonisation and proliferation can lead to infections that can delay the process [45, 46]. Therefore, in the assessment of the antibacterial effects of PAA in vivo, the *S. aureus* loading is

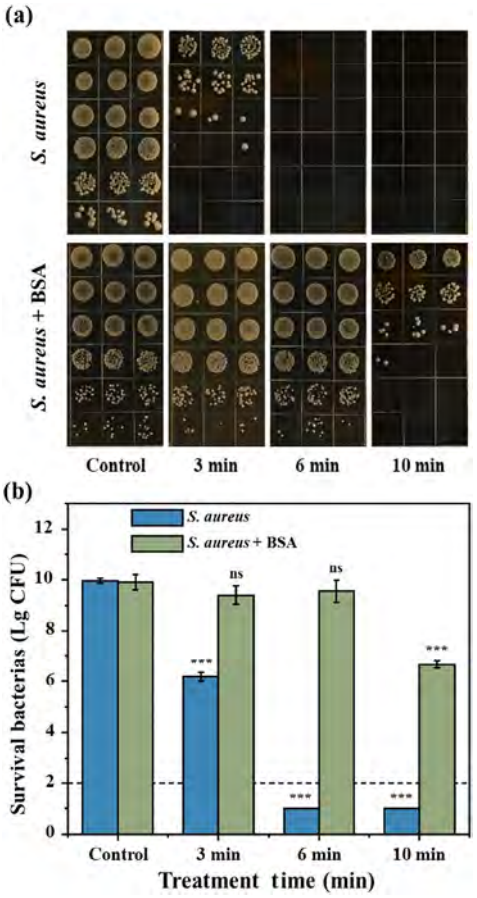


**FIGURE 5** | In vitro antibacterial effects of PAA: (a) bacteria growth on the TSB solid medium (each column represents an experimental sample [gradient dilution results], and each line represents the repeat experimental results) and (b) statistics of sterilisation effects ($n = 3$, $^{*}p < 0.05$, $^{**}p < 0.01$, $^{***}p < 0.001$).

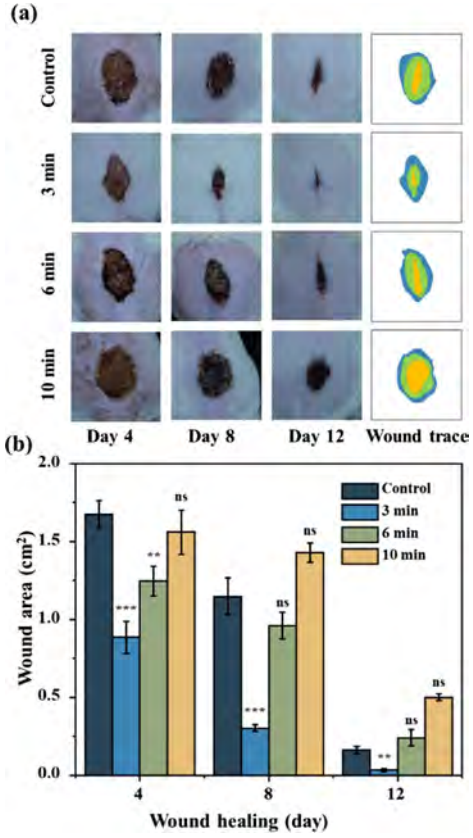


**FIGURE 6** | Wound pro-healing effects after different-dose PAA treatments: (a) photographs showing wound healing and (b) wound area statistics ($n = 5$, $^{*}p < 0.05$, $^{**}p < 0.01$, $^{***}p < 0.001$).

monitored. As shown in Figure 7a, there is a significant reduction in the *S. aureus* loading after the PAA treatment compared with the control group, and the antibacterial effects increase with the PAA treatment time. On the 2nd day of wound healing, the *S. aureus* counts on the wound surface of the PAA-10 min treatment group decrease by more than 95%, and more than 90% reduction is observed from the PAA-3 min treatment group compared to the control group (Figure 7b). However, on the 4th day, the *S. aureus* counts on the wound surface of the PAA-10 min decrease by more than 80% compared to about 50% for the PAA-3 min group. The difference diminishes probably because the penetration efficiency of reactive species in PAA to the wound tissues decreases for thicker wound scabs.

Although the PAA treatment cannot completely kill *S. aureus* on the wound surface, the bacterial loading of the infected wound decreases in a dose-dependent manner. It is well known that infections cause wound inflammation, and an excessive inflammatory response can impede wound healing [47]. Hence, immunohistochemical analysis is conducted on macrophages. On the 3rd day, an obvious inflammatory infiltration of mononuclear macrophages is observed from the control, PAA-6 min and PAA-10 min groups (Figure 7c), likely causing the wounds to heal slowly. In contrast, although there is also macrophage invasion, significantly fewer macrophages are observed from the PAA-3 min group than the other groups (Figure 7d). Therefore, the high doses used in the PAA-6 min and PAA-10 min treatments induce serious oxidative stress in the wound tissues while efficiently killing *S. aureus* on the surface, consequently causing severe inflammatory responses and hindering wound healing. Hence, only the low-dose PAA-3 min treatment can reduce inflammation while promoting wound healing.

After the inflammatory phase, cell growth factors such as FGF, EGF and VEGF, which are involved in the healing process to regulate epithelialisation, collagen accumulation and angiogenesis, play important roles in the remodelling process of wound healing. Immunohistochemical analysis is carried out to detect FGF, EGF and VEGF in the wound tissue. As shown in Figure 8, on the 6th day of wound healing, the rate of positive cells expressing FGF, EGF and VEGF in all three PAA treatment groups increases significantly compared to that of the control group, and the PAA-3 min treatment group shows more positive cells expressing FGF, EGF and VEGF. The production and release of FGF, EGF and VEGF aids wound healing, and our results show that the right dose promotes tissue repair and regeneration by inducing the production of cell growth factors during wound healing. However, the mechanism by which high-valence $NO_x$ in PAA regulates the expression of growth factors in wound tissues still needs to be clarified by future studies.

Finally, the biosafety of PAA is evaluated by histological analysis of the vital visceral tissues and blood biochemical

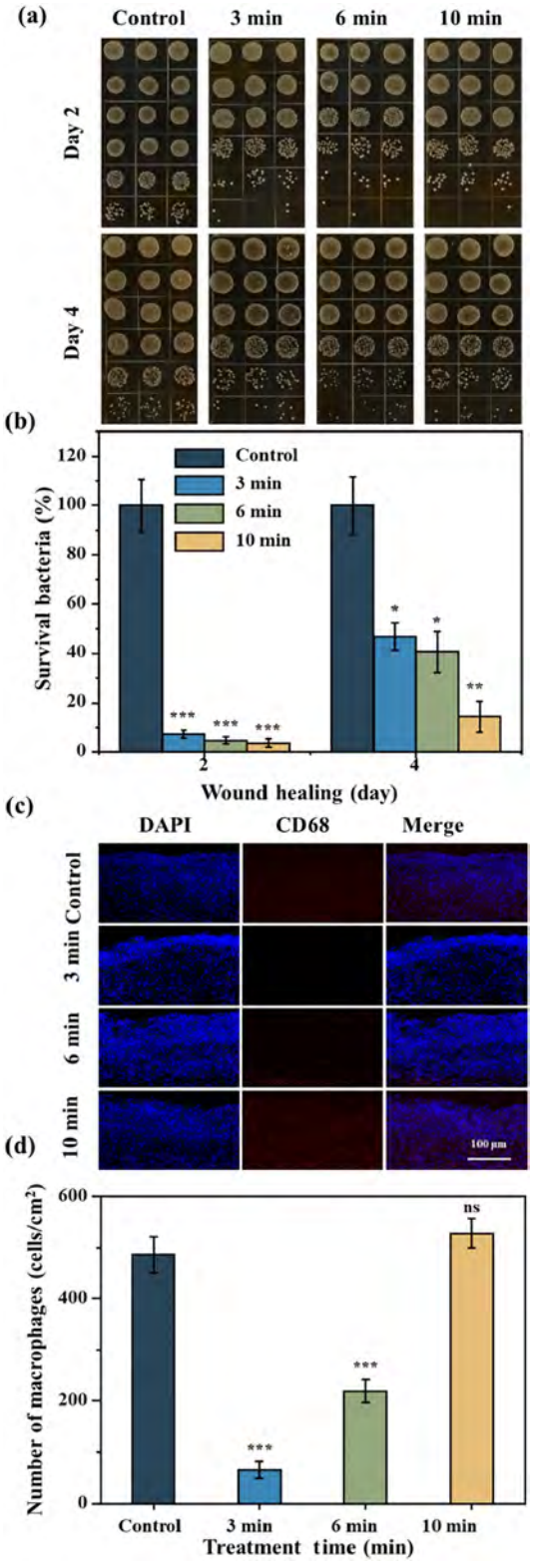


**FIGURE 7** | Inhibition effects of the PAA treatment on the wound bacterial loads and inflammation: (a) bacterial growth on the TSB solid medium (each column represents an experimental sample [gradient dilution results], and each line represents the repeat experimental results); (b) statistics of wound bacterial survival; (c) expression levels of CD68 by immunofluorescence staining; (d) statistics of the macrophage numbers ($n = 5$, $^{*}p < 0.05$, $^{**}p < 0.01$, $^{***}p < 0.001$).

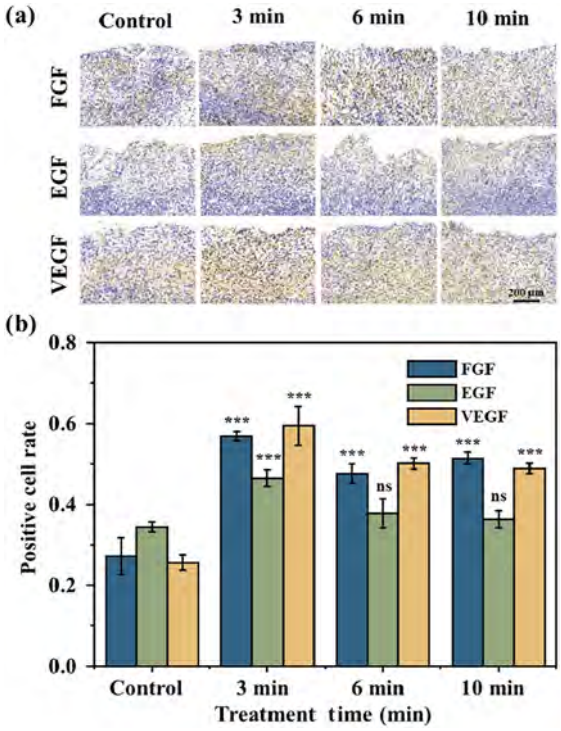


**FIGURE 8** | Immunohistochemical staining of growth factors: (a) immunohistochemical staining of FGF, EGF and VEGF and (b) statistics of the rates of FGF, EGF and VEGF positive cells ($n = 5$, $^{***}p < 0.001$).

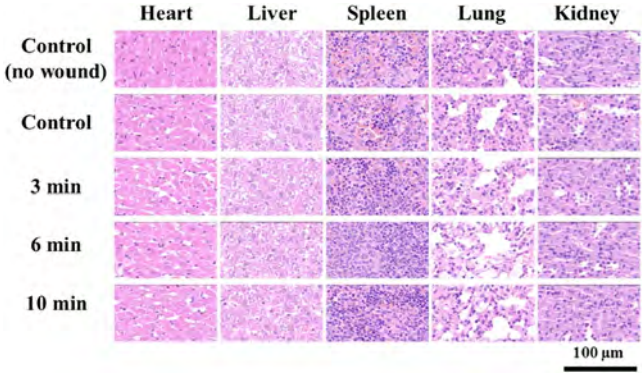


**FIGURE 9** | H&E staining histological analyses of the heart, liver, spleen, lung and kidney on the 6th day during wound healing.

parameters. The H&E staining results in Figure 9 show no obvious abnormal changes in the vital organs tissue structure and cell composition of the rats after the PAA treatment. The changes in the blood biomedical parameters after wound model construction and PAA treatment are shown in Table 2.

The number of white blood cells, lymphocytes, monocytes and granulocytes in the blood of rats with wounds increases compared with the control group without wounds. The rats treated with PAA for 3 min exhibited a smaller decrease in these cell types, indicating that PAA promotes the recovery of abnormal biochemical parameters in blood after wound formation. Considering these results, PAA treatment (no more than 10 min) shows no evident systemic toxicity in vivo.

**TABLE 2** | Effects of PAA on haematological parameters in rats.

| Parameter | Control-no wound | Control | PAA-3 min | PAA-6 min | PAA-10 min | Reference range |
|---|---|---|---|---|---|---|
| WBC($\times10^9$/L) | 6.83 ± 2.25 | 18.7 ± 9.05 | 11.63 ± 2.86 | 16.7 ± 14.05 | 25.23 ± 25.18 | 2.9–15.3 |
| Lymph ($\times10^9$/L) | 5.23 ± 1.92 | 10.77 ± 5.4 | 6.57 ± 1.82 | 10.33 ± 8.64 | 14.87 ± 15.43 | 2.6–13.5 |
| Mon ($\times10^9$/L) | 0.2 ± 0.1 | 1.17 ± 0.59 | 0.9 ± 0.36 | 0.67 ± 0.47 | 1.13 ± 0.93 | 0.0–0.5 |
| Gran ($\times10^9$/L) | 1.4 ± 0.26 | 6.77 ± 3.1 | 4.17 ± 0.78 | 5.7 ± 5.03 | 9.23 ± 8.82 | 0.4–3.2 |
| RBC ($\times10^{12}$/L) | 4.9 ± 0.19 | 4.99 ± 0.33 | 5.22 ± 0.76 | 4.8 ± 0.44 | 4.83 ± 0.9 | 5.6–7.89 |
| HGB (g/L) | 108.33 ± 2.31 | 112 ± 4.36 | 117 ± 15.13 | 103 ± 8.54 | 108 ± 14.42 | 120–150 |
| HCT (%) | 31.03 ± 1 | 32.07 ± 1.69 | 33.63 ± 4.44 | 29.6 ± 3.41 | 31.73 ± 5.54 | 36–46 |
| MCV (fL) | 63.47 ± 1.19 | 64.33 ± 3.44 | 64.67 ± 1.01 | 61.67 ± 1.5 | 65.97 ± 0.9 | 53–68.8 |
| MCH (pg) | 22.07 ± 0.42 | 22.4 ± 0.7 | 22.37 ± 0.42 | 21.4 ± 0.78 | 22.5 ± 1.49 | 16–23.1 |
| MCHC (g/L) | 348.67 ± 6.43 | 349 ± 11 | 347.33 ± 2.08 | 348.33 ± 14.01 | 342 ± 17.78 | 300–341 |
| RDW (%) | 13.2 ± 0.95 | 15.43 ± 0.71 | 14.07 ± 1.67 | 14.97 ± 1.45 | 15.3 ± 1.82 | 11–15.5 |
| PLT ($\times10^9$/L) | 477.33 ± 451.9 | 999 ± 447.83 | 1094.67 ± 527.8 | 617 ± 650.72 | 850.33 ± 441.82 | 100–1610 |
| MPV (fL) | 6.73 ± 0.32 | 6.5 ± 0.1 | 6.37 ± 0.21 | 7.33 ± 0.32 | 7.3 ± 0.61 | 3.8–6.2 |
| PDW | 17.5 ± 1.05 | 17 ± 0.17 | 16.67 ± 0.45 | 18.63 ± 1.58 | 17.67 ± 1.85 | / |
| PCT (%) | 0.31 ± 0.29 | / | 0.53 ± 0.2 | 0.19 ± 0.15 | / | / |

## 4 | Conclusions

A PAA therapeutic platform with higher biological activity is designed with the combination of a gliding arc discharge reactor and DBD discharge reactor and demonstrated for the treatment of infected wounds as an alternative to the conventional direct plasma treatment. In vitro experiments show that PAA can effectively inactivate the *S. aureus* suspension by producing aqueous reactive species. The in vivo experiments based on the *S. aureus* infected wound model reveal that although the high-dose treatments (PAA-6 in and PAA-10 min) reduce the bacterial loads and promote cytokine production, only the low-dose treatment (PAA-3 min) can inhibit macrophage invasion and inflammatory response and accelerate wound healing. The biosafety of the PAA treatment is confirmed by the rat model. The results show that the PAA treatment with the appropriate dose is a safe and effective clinical method for wound healing.

### Conflicts of Interest

The authors declare no conflicts of interest.

### Data Availability Statement

The authors confirm that the data supporting the findings of this study are available within the article.

### References


1. D. Chicharro-Alcántara, M. Rubio-Zaragoza, E. Damiá-Giménez, et al., "Platelet Rich Plasma: New Insights for Cutaneous Wound Healing Management," *Journal of Functional Biomaterials* 9, no. 1 (2018): 10.

2. A. C. D. O. Gonzalez, T. F. Costa, Z. d. Andrade, and A. R. A. P. Medrado, "Wound Healing—A Literature Review," *Anais Brasileiros de Dermatologia* 91, no. 5 (2016): 614–620.

3. S. Guo and L. DiPietro, "Factors Affecting Wound Healing," *Journal of Dental Research* 89, no. 3 (2010): 219–229.

4. C. M. Lamb and J. Garner, "Selective Non-Operative Management of Civilian Gunshot Wounds to the Abdomen: A Systematic Review of the Evidence," *Injury* 45, no. 4 (2014): 659–666.

5. K. C. Soares, P. A. Baltodano, C. W. Hicks, et al., "Novel Wound Management System Reduction of Surgical Site Morbidity After Ventral Hernia Repairs: A Critical Analysis," *American Journal of Surgery* 209, no. 2 (2015): 324–332.

6. B. H. J. Gowda, S. Mohanto, A. Singh, et al., "Nanoparticle-Based Therapeutic Approaches for Wound Healing: A Review of the State-of-the-Art," *Materials Today Chemistry* 27 (2023): 101319.

7. T. Zhang, F. Liu, and W. Tian, "Advance of New Dressings for Promoting Skin Wound Healing," *Journal of Biomedical Engineering* 36, no. 6 (2019): 1055–1059.

8. S. Emmert, A. van Welzen, K. Masur, et al., "Kaltes Atmosphärendruckplasma zur Behandlung akuter und chronischer Wunden," *Hautarzt* 71, no. 11 (2020): 855–862.

9. T. Shao, C. Zhang, R. Wang, et al., "Atmospheric-Pressure Pulsed Gas Discharge and Pulsed Plasma Application", *High Voltage Engineering* 42 (2016): 685–705 (in Chinese).

10. E. Robert, T. Darny, S. Dozias, S. Iseni, and J. M. Pouvesle, "New Insights on the Propagation of Pulsed Atmospheric Plasma Streams: From Single Jet to Multi Jet Arrays," *Physics of Plasmas* 22, no. 12 (2015): 122007.

11. L. Guo, P. Zhao, Y. Jia, et al., "Inactivation of Airborne Pathogenic Microorganisms by Plasma-Activated Nebulized Mist," *Journal of Hazardous Materials* 459 (2023): 132072.

12. L. Guo, R. Xu, L. Gou, et al., "Mechanism of Virus Inactivation by Cold Atmospheric-Pressure Plasma and Plasma-Activated Water," *Applied and Environmental Microbiology* 84, no. 17 (2018): e00726–e00818.

13. M. Keidar, A. Shashurin, O. Volotskova, et al., "Cold Atmospheric Plasma in Cancer Therapy," *Physics of Plasmas* 20, no. 5 (2013): 057101.

14. T. Fang, X. Cao, B. Shen, Z. Chen, and G. Chen, "Injectable Cold Atmospheric Plasma-Activated Immunotherapeutic Hydrogel for Enhanced Cancer Treatment," *Biomaterials* 300 (2023): 122189.

15. J. Heinlin, G. Isbary, W. Stolz, et al., "Plasma Applications in Medicine With a Special Focus on Dermatology," *Journal of the European Academy of Dermatology and Venereology* 25, no. 1 (2011): 1–11.

16. H. Chen, X. Tang, Y. Huang, et al., "Remodel the Perifollicular Microenvironment via Minoxidil-Loaded Microneedle Patch and Cold Atmospheric Plasma for Treating Androgenetic Alopecia," *Nano Research* 17, no. 7 (2024): 6411–6419.

17. V. Vijayarangan, A. Delalande, S. Dozias, J. M. Pouvesle, E. Robert, and C. Pichon, "New Insights on Molecular Internalization and Drug Delivery Following Plasma Jet Exposures," *International Journal of Pharmaceutics* 589 (2020): 119874.

18. T. Maho, R. Binois, F. Brulé-Morabito, et al., "Anti-Bacterial Action of Plasma Multi-Jets in the Context of Chronic Wound Healing," *Applied Science* 11, no. 20 (2021): 9598.

19. F. Brehmer, H. Haenssle, G. Daeschlein, et al., "Alleviation of Chronic Venous Leg Ulcers With a Hand-Held Dielectric Barrier Discharge Plasma Generator (PlasmaDerm VU-2010): Results of a Monocentric, Two-Armed, Open, Prospective, Randomized and Controlled Trial (NCT01415622)," *Journal of the European Academy of Dermatology and Venereology* 29, no. 1 (2015): 148–155.

20. S. K. Dubey, S. Parab, A. Alexander, et al., "Cold Atmospheric Plasma Therapy in Wound Healing," *Process Biochemistry* 112 (2022): 112–123.

21. S. A. Ermolaeva, A. F. Varfolomeev, M. Y. Chernukha, et al., "Bactericidal Effects of Non-Thermal Argon Plasma In Vitro, in Biofilms and in the Animal Model of Infected Wounds," *Journal of Medical Microbiology* 60, no. 1 (2011): 75–83.

22. G. Daeschlein, M. Napp, S. von Podewils, et al., "In Vitro Susceptibility of Multidrug Resistant Skin and Wound Pathogens Against Low Temperature Atmospheric Pressure Plasma Jet (APPJ) and Dielectric Barrier Discharge Plasma (DBD)," *Plasma Processes and Polymers* 11, no. 2 (2014): 175–183.

23. J. L. Zimmermann, T. Shimizu, H. U. Schmidt, Y. F. Li, G. E. Morfill, and G. Isbary, "Test for Bacterial Resistance Build-Up Against Plasma Treatment," *New Journal of Physics* 14, no. 7 (2012): 073037.

24. C. Dunnill, T. Patton, J. Brennan, et al., "Reactive Oxygen Species (ROS) and Wound Healing: The Functional Role of ROS and Emerging ROS-Modulating Technologies for Augmentation of the Healing Process," *International Wound Journal* 14, no. 1 (2017): 89–96.

25. M. J. Malone-Povolny, S. E. Maloney, and M. H. Schoenfisch, "Nitric Oxide Therapy for Diabetic Wound Healing," *Advanced Healthcare Materials* 8, no. 12 (2019): 1801210.

26. Z. Wang, L. Liu, D. Liu, et al., "Combination of $NO_x$ Mode and $O_3$ Mode Air Discharges for Water Activation to Produce a Potent Disinfectant," *Plasma Sources Science and Technology* 31, no. 5 (2022): 05LT01.

27. J. He, Z. Li, J. Wang, et al., "Photothermal Antibacterial Antioxidant Conductive Self-Healing Hydrogel With Nitric Oxide Release Accelerates Diabetic Wound Healing," *Composites Part B: Engineering* 266 (2023): 110985.

28. D. Liu, T. He, and H. Zhang, "Penetration Effect of Gas Plasmas on Human Tissues: State-of-the-Art and Current Issues", *High Voltage Engineering* 45, no. 7 (2019): 2329–2342 (in Chinese).

29. L. S. Rothman, I. Gordon, A. Barbe, et al., "The HITRAN 2008 Molecular Spectroscopic Database," *Journal of Quantitative Spectroscopy & Radiative Transfer* 110, no. 9–10 (2009): 533–572.

30. Z. Wang, Y. Qi, L. Guo, et al., "The Bactericidal Effects of Plasma-Activated Saline Prepared by the Combination of Surface Discharge Plasma and Plasma Jet," *Journal of Physics D Applied Physics* 54, no. 38 (2021): 385202.

31. I. B. Gosbell, "The Significance of MRSA and VRE in Chronic Wounds. Prim. Intent," *Australian Journal of Wound Management* 10, no. 1 (2002): 15–19.

32. S. Y. Wong, R. Manikam, and S. Muniandy, "Prevalence and Antibiotic Susceptibility of Bacteria From Acute and Chronic Wounds in Malaysian Subjects," *Journal of Infection in Developing Countries* 9, no. 9 (2015): 936–944.

33. A. F. Cardona and S. E. Wilson, "Skin and Soft-Tissue Infections: A Critical Review and the Role of Telavancin in Their Treatment," supplement, *Clinical Infectious Diseases* 61, no. S2 (2015): S69–S78.

34. W. Xia, D. Liu, L. Guo, et al., "Discharge Characteristics and Bactericidal Mechanism of Ar Plasma Jet With Ethanol and Oxygen Gas Admixtures," *Plasma Sources Science and Technology* 28, no. 12 (2019): 125005.

35. S. Park, W. Choe, and C. Jo, "Interplay Among Ozone and Nitrogen Oxides in Air Plasmas: Rapid Change in Plasma Chemistry," *Chemical Engineering Journal* 352 (2018): 1014–1021.

36. J. J. Lowke and R. Morrow, "Theoretical Analysis of Removal of Oxides of Sulphur and Nitrogen in Pulsed Operation of Electrostatic Precipitators," *IEEE Transactions on Plasma Science* 23, no. 4 (1995): 661–671.

37. Z. Wang, M. Zhu, D. Liu, et al., "$N_2O_5$ in Air Discharge Plasma: Energy-Efficient Production, Maintenance Factors and Sterilization Effects," *Journal of Physics D Applied Physics* 56, no. 7 (2023): 075204.

38. R. Zhou, P. Wang, Y. Xian, et al., "Plasma-Activated Water: Generation, Origin of Reactive Species and Biological Applications," *Journal of Physics D Applied Physics* 53, no. 30 (2020): 303001.

39. C. C. W. Verlackt, W. Van Boxem, and A. Bogaerts, "Transport and Accumulation of Plasma Generated Species in Aqueous Solution," *Physical Chemistry Chemical Physics* 20, no. 10 (2018): 6845–6859.

40. S. Ikawa, K. Kitano, and S. Hamaguchi, "Effects of pH on Bacterial Inactivation in Aqueous Solutions Due to Low-Temperature Atmospheric Pressure Plasma Application," *Plasma Processes and Polymers* 7, no. 1 (2010): 33–42.

41. P. Lukes, E. Dolezalova, I. Sisrova, and M. Clupek, "Aqueous-Phase Chemistry and Bactericidal Effects From an Air Discharge Plasma in Contact With Water: Evidence for the Formation of Peroxynitrite through a Pseudo-Second-Order Post-discharge Reaction of $H_2O_2$ and $HNO_2$," *Plasma Sources Science and Technology* 23, no. 1 (2014): 015019.

42. G. Collet, E. Robert, A. Lenoir, et al., "Plasma Jet-Induced Tissue Oxygenation: Potentialities for New Therapeutic Strategies," *Plasma Sources Science and Technology* 23, no. 1 (2014): 184–195.

43. P. Di Simplicio, K. H. Cheeseman, and T. F. Slater, "The Reactivity of the SH Group of Bovine Serum Albumin With Free Radicals," *Free Radical Research Communications* 14, no. 4 (1991): 253–262.

44. G. Scorza and M. Minetti, "One-Electron Oxidation Pathway of Thiols by Peroxynitrite in Biological Fluids: Bicarbonate and Ascorbate Promote the Formation of Albumin Disulphide Dimers in Human Blood Plasma," *Biochemical Journal* 329, no. 2 (1998): 405–413.

45. G. C. Gurtner, S. Werner, Y. Barrandon, and M. T. Longaker, "Wound Repair and Regeneration," *Nature* 453, no. 7193 (2008): 314–321.

46. B. Haertel, T. v. Woedtke, K. D. Weltmann, and U. Lindequist, "Non-Thermal Atmospheric-Pressure Plasma Possible Application in Wound Healing," *Biomolecules & Therapeutics* 22, no. 6 (2014): 477–490.

47. C. Y. Zou, X. X. Lei, J. J. Hu, et al., "Multi-Crosslinking Hydrogels With Robust Bio-Adhesion and Pro-Coagulant Activity for First-Aid Hemostasis and Infected Wound Healing," *Bioactive Materials* 16 (2022): 388–402.